

# Geophysical Research Letters



### **RESEARCH LETTER**

10.1029/2022GL102186

#### **Key Points:**

- · Observations show a boomerang-shape aerosol effect on the top height of convective precipitation from invigoration to suppression
- Aerosols impose distinct effects on precipitation rate at different layers, with no significant impact near surface
- Energy change within conversion processes between hydrometeors and water vapor explains different responses of precipitation to aerosol

#### **Supporting Information:**

Supporting Information may be found in the online version of this article.

#### Correspondence to:

C. Zhao. cfzhao@pku.edu.cn

#### Citation:

Sun, Y., Wang, Y., Zhao, C., Zhou, Y., Yang, Y., Yang, X., et al. (2023). Vertical dependency of aerosol impacts on local scale convective precipitation. Geophysical Research Letters, 50, e2022GL102186. https://doi. org/10.1029/2022GL102186

Received 21 NOV 2022 Accepted 7 JAN 2023

#### **Author Contributions:**

Conceptualization: Yue Sun Data curation: Yue Sun

Formal analysis: Yue Sun, Yuan Wang, Chuanfeng Zhao, Yue Zhou, Yikun Yang, Xingchuan Yang, Hao Fan, Xin Zhao,

Jie Yang

Funding acquisition: Chuanfeng Zhao Investigation: Chuanfeng Zhao,

Yikun Yang

Methodology: Yue Sun, Yuan Wang,

Chuanfeng Zhao

Supervision: Chuanfeng Zhao Validation: Xingchuan Yang Visualization: Yue Sun, Yikun Yang

#### © 2023 The Authors.

This is an open access article under the terms of the Creative Commons Attribution-NonCommercial License, which permits use, distribution and reproduction in any medium, provided the original work is properly cited and is not used for commercial purposes.

## **Vertical Dependency of Aerosol Impacts on Local Scale Convective Precipitation**

Yue Sun<sup>1</sup>, Yuan Wang<sup>2</sup>, Chuanfeng Zhao<sup>1,3</sup>, Yue Zhou<sup>1</sup>, Yikun Yang<sup>1,3</sup>, Xingchuan Yang<sup>1,4</sup>, Hao Fan<sup>1</sup> D, Xin Zhao<sup>1</sup>, and Jie Yang<sup>1</sup>

<sup>1</sup>College of Global Change and Earth System Science, Beijing Normal University, Beijing, China, <sup>2</sup>Department of Earth, Atmospheric, and Planetary Sciences, Purdue University, West Lafayette, IN, USA, 3Department of Atmospheric and Oceanic Sciences, School of Physics, Peking University, Beijing, China, <sup>4</sup>College of Resource Environment and Tourism, Capital Normal University, Beijing, China

**Abstract** Aerosol effects on convective precipitation is critical for understanding human impacts on extreme weather and the hydrological cycle. However, even their signs and magnitude remain debatable. In particular, aerosol effects on vertical structure of precipitation have not been systematically examined yet. Combining 6-year space-borne and ground-based observations over the North China Plain, we show a boomerang-shape aerosol effect on the top height of convective precipitation, from invigoration to suppression. Further analyses reveal that the aerosols play distinct effects on precipitation rate at different layers. Particularly, near surface precipitation rate shows no significant responses to aerosol and precipitation-top height due to strong evaporation. The competition of energy between released from condensation and freezing and absorbed by evaporation contributes to different responses of precipitation-top height to aerosol and can explain the boomerang-shape aerosol effect.

Plain Language Summary Aerosol particles in the atmosphere can alter precipitation efficiency and modulate the hydrological cycle, while their impacts on the cloud and precipitation vertical profiles remain poorly understood. Using 6-year multi-source observation data along with reanalysis meteorology, we find that aerosols exert distinct effects on precipitation rate at different layers. The observations show that aerosols enhance precipitation-top height first and then suppress it under various dynamics and thermodynamics conditions, with a turning point at medium aerosol amount. In contrast, the response of near surface precipitation rate to aerosol perturbation is complex due to varying evaporation efficiency. These findings challenge the previous studies that suggested that the characteristics of cloud and precipitation at high altitude are closely correlated with precipitation rate near the surface.

#### 1. Introduction

Precipitation is a fundamental driver of the global hydrological cycle and has profound implications on human life and social society (Ramanathan et al., 2001; Swain et al., 2018; Wang L et al., 2021; Zhang et al., 2021). It can shorten cloud lifetime, regulate cloud water content and then affect radiative energy budget (Ackerman et al., 2000; Albrecht, 1989; Twomey, 1977). The aerosol effects on precipitation are complicated and have raised much attention. Aerosol microphysical and radiative effects have critical influence on cloud and precipitation (Ackerman et al., 2000; Albrecht, 1989; Twomey, 1977; Wang F. et al., 2018; Wang Y. et al., 2018). Diverse aerosol effects have been found in previous studies, debating on whether aerosol effects are significant (Guo J. et al., 2014), whether the effects are suppression (Ackerman et al., 2000; Kaufman & Fraser, 1997; Kaufman & Nakajima, 1993; Qian et al., 2009; Rosenfeld, 1999; Zhao et al., 2006) or enhancement (Fan et al., 2018; Koren et al., 2005; Rosenfeld et al., 2008; Wang et al., 2016; Zhao et al., 2018), and whether the effects are monotonic (Guo X. L. et al., 2014; Jiang et al., 2016; Koren et al., 2008; Liu H. et al., 2019; Yang et al., 2018). The dynamics, thermodynamics (Fan et al., 2009; Guo J. et al., 2016; Sun & Zhao, 2020, 2021; Xiao et al., 2022), aerosol types (Han et al., 2022; Jiang et al., 2018; Yang et al., 2016) and cloud types (Chen et al., 2016; Garrett & Zhao, 2006; Gryspeerdt et al., 2014; Gryspeerdt & Stier, 2012) can all modify the aerosol effect on cloud and precipitation.

Aerosols in the cloud and under the cloud play distinguishable effects on precipitation. In the cloud, the aerosols can affect cloud particle effective radius, evaporation rates, condensation and coalescence efficiency and then the competition of latent heat between released and absorbed (Jiang et al., 2006; Lee et al., 2015), which

SUN ET AL. 1 of 11 Writing – original draft: Yue Sun Writing – review & editing: Yuan Wang Chuanfeng Zhao can cause further influence on cloud and precipitation, especially for the precipitation with ice-phase processes (Andreae et al., 2004; Fan et al., 2018; Lin et al., 2006; Rosenfeld et al., 2008). Under the cloud, absorbing aerosols can modify the atmospheric thermodynamic structure (Wang et al., 2013), water vapor environment (Sun & Zhao, 2020), and then precipitation, especially the evaporation process, which has not been highlighted yet in previous studies.

Most previous studies have investigated aerosol effect on precipitation by studying the relationships between aerosol and surface precipitation rate or characteristics of cloud (Jiang et al., 2016; Xiao et al., 2022), but few have analyzed the topic from the perspective of the whole vertical structure. The global precipitation measurement (GPM) mission dual-frequency precipitation radar (DPR) data set (GPM-DPR) provides precipitation rate profile and precipitation types (convective, stratiform, and other), while the data set are mainly used to study the vertical structure of precipitation (Sun et al., 2020; Wang R et al., 2021; Yang et al., 2021a) without considering aerosol impacts. Several studies have used GPM-DPR data set to study the aerosol effect on precipitation, but still focused on surface precipitation rate (Xiao et al., 2022).

Here, we use precipitation rate, including GPM precipitation rate profile and hourly China Merged Precipitation Analysis product (CMPA), surface PM<sub>2.5</sub> mass concentration, solid/liquid precipitation water in column from GPM, convective available potential energy (CAPE) from the National Centers for Environmental Prediction (NCEP), precipitable water vapor (PWV) from MERRA-2, wind shear (WS) and relative humidity (RH) from ERA5 to examine the aerosol effect on precipitation-top height and the near surface precipitation rate. With these data, we here address the question: How do aerosols affect precipitation rate at different layers, along with the potential reasons behind?

#### 2. Data and Method

The study region is located at 113.4°-120.0°E, 35.0°-41.0°N with the altitude of 0–2 km above sea level (Figure 1a), which has attracted much interest with serious air pollution and dense population, even though air quality over this region has been improved gradually and significantly during past decade (Fan et al., 2021; Guo J. et al., 2014; Sun et al., 2022; Zhang et al., 2020). The aerosol effects on precipitation may be different over the mountainous and plain regions, so this study only selects the area with Digital Elevation Model (DEM) less than 100 m (Chen et al., 2021; Guo J. et al., 2014; Yang et al., 2021b, 2021c). The study period focuses on the warm season (May to September) of multiple years from 2015 to 2020. Detailed information about the precipitation, aerosol, meteorology, and cloud data adopted in this study are shown in Table S1 in Supporting Information S1.

The Ku-/Ka-band DPR from GPM can detect precipitation properties effectively and then provide rich precipitation information, such as precipitation types, precipitation top height, precipitation rate, and so on, which have been validated and widely used in previous studies (e.g., Hamada & Takayabu, 2015; Kotsuki et al., 2014; Sun et al., 2020; Zhang & Fu, 2018). The convective precipitation is more sensitive to aerosol compared to stratiform precipitation and the ice-phase process of precipitation has been highlighted in many recent studies (Li et al., 2022; Mülmenstädt et al., 2015; Sun & Zhao, 2021), so we focus our study on the convective precipitation with ice-process. We only choose the cases that the precipitation-top height is above the freezing level to confirm the existence of ice processes. We focus on the responses of precipitation-top height and precipitation rate to aerosols. Note that we remove the extreme heavy precipitation events with precipitation rates over 10 mm hr<sup>-1</sup>.

The different types of aerosols have different influence on cloud and precipitation (Han et al., 2022; Jiang et al., 2018; Sun & Zhao, 2021). We use single scattering albedo (SSA, 440 nm) and fine mode fraction (FMF, 500 nm) from the AEROSOL ROBOTIC NETWORK (AERONET) (Lee et al., 2010) to investigate the aerosol types. As shown in Figure S1 in Supporting Information S1, the SSA is from 0.90 to 0.95 and the FMF is from 0.60 to 0.84, which means that the slightly-absorbing fine mode aerosols are dominant in the study region during our study period. Considering this, we have not further refined the aerosol types. Compared to AOD and coarse mode aerosol concentrations, fine mode aerosol mass concentration can better serve as the proxy for cloud condensation nuclei (CCN) (Pan et al., 2021), so we use the mean PM<sub>2.5</sub> mass concentration within 4 hr before precipitation to represent the amount of CCN, which can weaken the influence of diurnal variations of aerosols (Sun & Zhao, 2021). The local scale convective precipitation meets the following criteria (Guo J. et al., 2019): (a) the precipitation start time is limited from 7:00-19:00 LT; (b) the proportion of rainy grids within a 15-grids radius around the selected grid has to be equal or less than 25%; (c) the proportion of rainy grids within a

SUN ET AL. 2 of 11

19448007, 2023, 2, Downloaded from https://agupubs.onlinelibrary.wiley.com/doi/10.1029/2022GL102186, Wiley Online Library on [19/01/2023]. See the Terms and Conditions (https://onlinelibrary.wiley.com/terms-and-con

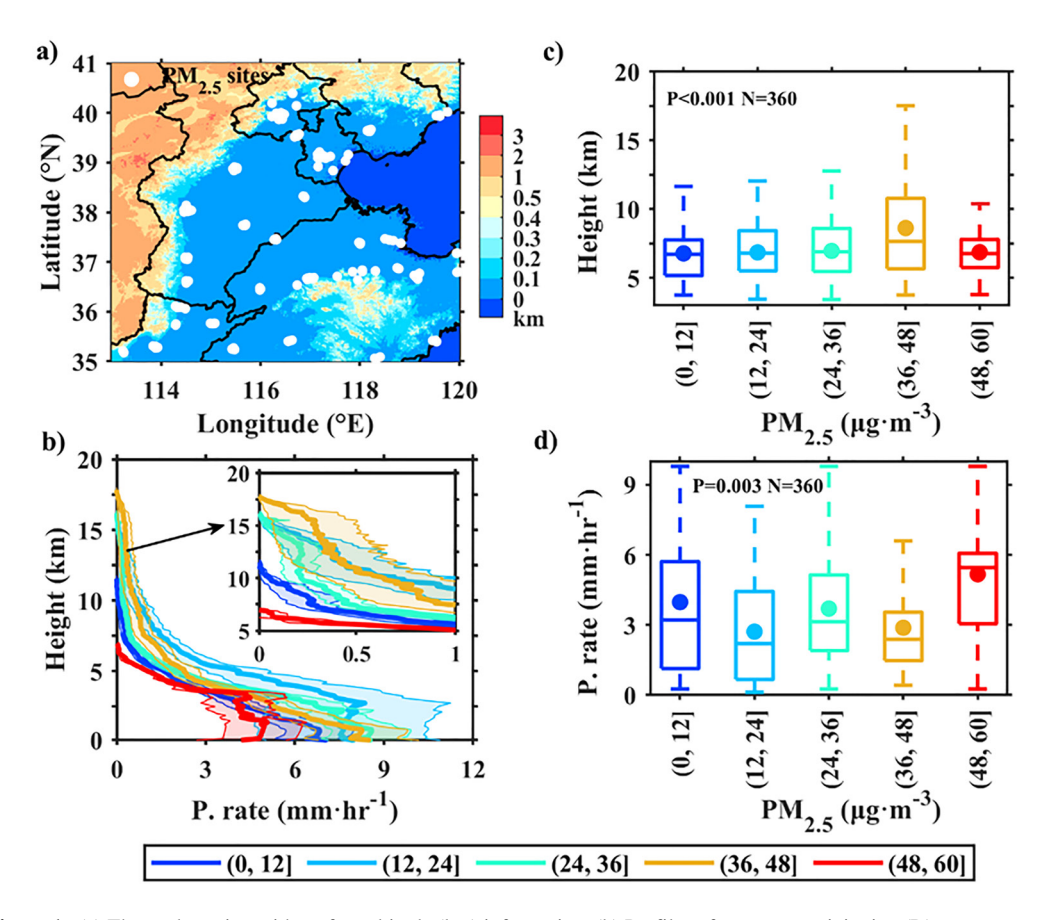


**Figure 1.** (a) The study region with surface altitude (km) information, (b) Profiles of average precipitation (P.) rate (mm hr<sup>-1</sup>), (c) the precipitation-top height (km) statistics, and (d) the near surface precipitation rate statistics for different ranges of PM<sub>2.5</sub> mass concentration in warm season (May-September) during 2015–2020 at North China Plain. The sample number (N) is 360. The colors of line from blue to red in (a) represent different PM<sub>2.5</sub> mass concentration with an interval of 12  $\mu$ g m<sup>-3</sup> from 0 to 60  $\mu$ g m<sup>-3</sup>. The *p*-value is from one-way ANOVA and the hypothesis is that all groups are drawn from populations with the same mean. The white dots in panel (a) represent the PM<sub>2.5</sub> site stations used in this study.

5-grids radius has to be equal or less than 50%; (d) the duration of precipitation event is less than 4 hr (Sun & Zhao, 2021). Note that a grid is with the spatial resolution of  $0.1 \times 0.1^{\circ}$ . We use the Aerosol Index (AI) from the Ozone Monitoring Instrument (OMI) onboard the Aura satellite to further investigate absorbing aerosol effect on precipitation. The positive (negative) AI values represent that the absorbing (scattering) aerosols are dominant in this region (Tariq & Ali, 2015). We remove the data with values from -0.1 to 0.1 due to potential large uncertainties (Hammer et al., 2018).

Previous studies have indicated that the dynamics and thermodynamics of atmospheric environment can significantly modify the aerosol effect on cloud and precipitation (Fan et al., 2009; Pan et al., 2021; Sun & Zhao, 2020). Here, we use the CAPE and WS to limit the impacts of dynamics and thermodynamics and use the PWV and RH to represent the moisture condition (e.g., Fan et al., 2009; Pan et al., 2021). Wind shear is calculated by max(u) minus min(u) within 400 hPa from 1,000 hPa (Fan et al., 2009). Relative humidity is defined with the averaged RH over 500–900 hPa (Fan et al., 2009). We group all data into two groups with similar meteorological conditions, which are High CAPE-High PWV-Low WS-High RH, and Low CAPE-Low PWV- High WS-Low RH.

Based on the nearest method in space, we first match  $PM_{2.5}$  and precipitation from the GPM with the distance less than 35 km. The locations of GPM observed precipitation properties will be matched with a grid point in CMPA, NCEP, MERRA-2, ERA5, and Himawari-8 and then get corresponding parameters from those datasets, including precipitation rate, CAPE, PWV, WS, RH, and cloud effective radius ( $r_e$ ). The time-continuous precipitation rates are provided by the CMPA, based on which we can obtain start time and duration of precipitation. Note that the start time and duration of precipitation are defined as the time when precipitation occurs and the time length from

SUN ET AL. 3 of 11

19448007, 2023, 2, Downloaded from https://agupubs.onlinelibrary.wiley.com/doi/10.1029/2022GL102186, Wiley Online Library on [19/01/2023]. See the Terms and Conditions (https://onlinelibrary

and-conditions) on Wiley Online Library for rules of use; OA articles are governed by the applicable Creative Commons Licenso

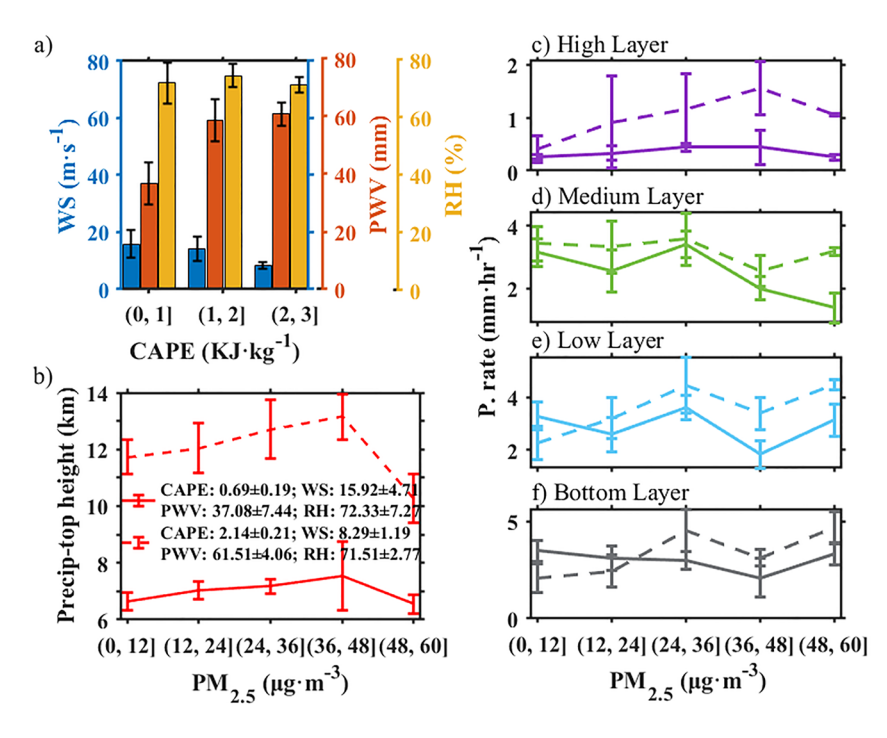


**Figure 2.** (a) The variations of wind shear (WS, m s<sup>-1</sup>; blue bar), precipitable water vapor (PWV, mm; orange bar) and relative humidity (RH, %; yellow bar) with convective available potential energy (CAPE, KJ kg<sup>-1</sup>); and the variations of (b) the precipitation-top height (km) statistics, (c) precipitation rate in High Layer statistics, (d) precipitation rate in Medium Layer statistics, (e) precipitation rate in Low Layer statistics, and (f) precipitation rate in Bottom Layer statistics for different ranges of PM<sub>2.5</sub> mass concentration under different meteorological conditions in warm season (May-September) during 2015–2020 at North China Plain. The solid and dashed lines represent different meteorological conditions as shown in panel (b).

precipitation occurrence to the end, respectively. Temporally, the CAPE and WS used are before precipitation start time, while the PWV and RH are matched with GPM precipitation time.

The cluster analysis is used to investigate the aerosol effect on precipitation. We find the similar results with different  $PM_{2.5}$  mass concentration intervals (Figure S2 in Supporting Information S1). Considering the limited sample volume, we investigate the aerosol effect on precipitation further with  $PM_{2.5}$  mass concentration interval of 12  $\mu$ g m<sup>-3</sup> from 0 to 60  $\mu$ g m<sup>-3</sup>. Note that the sample number in every bin is set more than 30 to ensure the validity of the statistics (Wilks, 2011).

#### 3. Results

#### 3.1. The Boomerang-Shape Aerosol Effect on Top Height of Convective Precipitation

The North China Plain (NCP) with a large range of aerosol concentration is an ideal place to investigate the aerosol effect on precipitation (Liu H et al., 2019). We focus on the local scale convective precipitation with ice-phase processes and find that the aerosol effect on precipitation-top height is not monotonic and varies from invigoration to suppression (Figures 1b and 1c). As shown in Figure 1c, the precipitation-top height is enhanced when PM<sub>2.5</sub> increases before reaching 36 μg m<sup>-3</sup> but suppressed when PM<sub>2.5</sub> changes from 36 to 60 μg m<sup>-3</sup> significantly. The aerosol effects on precipitation-top height shown in Figure 1c may be linked with covarying meteorological conditions (Koren et al., 2012; Pan et al., 2021). As shown in Figure 2a, the meteorological factors are coupled. The high (low) CAPE is accompanied with high (low) PWV and low (high) WS and the RHs are similar under different CAPE conditions. We further examine the potential influence of CAPE, PWV, WS, and RH on precipitation in Figure 2b. The boomerang-shape effects from invigoration to suppression are shown in Figure 2b with similar PM<sub>2.5</sub> turning points under different meteorological conditions, that are 36–48 μg m<sup>-3</sup>. The competition of latent heat between released by condensation/freezing and absorbed by evaporation can help explain the boomerang-shape effects of aerosols on precipitation and will be shown in detail in the theoretical hypothesis proposed in Section 3.3. The conducive dynamics conditions with high CAPE and low WS and abundant supply

SUN ET AL. 4 of 11

of water vapor with high PWV and RH can enhance the precipitation-top height evidently. In a word, the aerosol can strengthen precipitation-top height first and then suppress it from clean to polluted conditions, and the atmospheric dynamics and moisture are important meteorological factors that can influence the aerosol effect on precipitation-top height.

#### 3.2. The Strong Evaporation Suppressing the Near Surface Precipitation Rate

It has been suggested that the characteristics of cloud and precipitation at high altitude are closely correlated with precipitation rate near the surface (Dagan et al., 2015; A. P. Khain, 2009; Li et al., 2008; Rosenfeld et al., 2008). However, the results from Figure 1d suggest an insignificant effect on near surface precipitation rate by aerosols, different from the responses of precipitation-top height. To explore the reasons, we examine the response of precipitation rate to aerosols at heights below and above the freezing levels, respectively, and the latter is linked with the net effect of complex mixed-phase cloud processes. The climatological freezing levels are  $4.8 \ (\pm 0.6)$  km in the study region. We divide the precipitation rates from freezing level to ground into three groups based on the same sample number, called as Medium Layer ( $\sim 3.2$ –4.8 km), Low Layer ( $\sim 1.6$ –3.2 km), and Bottom Layer ( $\sim 0$ –1.6 km) from high (freezing level) to low (near surface) in altitudes and the High Layer is from precipitation-top height to freezing level.

Figure 2c shows that the precipitation-top height can influence precipitation rates above freezing level under different meteorological conditions. While, the precipitation rate shows insignificant responses to aerosol below the freezing level (shown in Figures 2d–2f), which indicates that the aerosol effect on precipitation is offset by other factors during falling. Being close to the surface, the temperature increases gradually and humidity conditions become complex, which are closely related to the intensity of evaporation. Thus, we further investigate the evaporation efficiency near the surface to understand this phenomenon.

We define a precipitation lapse rate by calculating the slope between precipitation rate and altitude in Medium Layer, Low Layer, and Bottom Layer, respectively, which can reflect the evaporation efficiency indirectly (Zhao & Garrett, 2008). The positive lapse rate indicates that the precipitation rate is further weakened in the process of precipitation falling, suggesting the evident role of evaporation. The percentages of the cases with significant correlations at a confidence level of 95% are 63%-83% (shown in Table S2 in Supporting Information S1). Both precipitation intensity and pollution conditions show different effects on lapse rates at different layers. The precipitation rates change evidently in Medium Layer, with rapidly increasing precipitation rate for 61%-93% cases, especially for heavy precipitation, which suggests that the evaporation is not dominant in Medium Layer (shown in Figures 3a, 3d and 3g). With precipitation falling, the proportions of cases that evaporation dominates increase gradually under different precipitation and pollution conditions at Low Layer (shown in Figure 3b). At the Bottom Layer, the evaporation is pre-dominant, and precipitation rates decrease for 59%-75% cases. Figures 3a-3c indicate that the proportions of the cases with evaporation dominant increase gradually as the precipitation approaches the ground (from Medium to Bottom Layer), which implies that evaporation can modify precipitation rate near the surface and then make the results of aerosol effects on precipitation rate near the surface not clear. Thus, the near surface precipitation rates are influenced by precipitation-top height, evaporation and other meteorological factors.

We investigate the liquid and solid precipitation water in column under different pollution and near surface precipitation rate conditions and find that the raindrop size and ice particle number contribute to the differences of lapse rate between light and heavy precipitation. Under the similar pollution conditions (assumed similar CCN number), the precipitation water in column is larger under heavy precipitation due to larger raindrop size (Figure 4a). The larger the size, the stronger the total evaporation is. While, the heavy precipitation is often along with more ice water (Figure 4a), which can cool the atmosphere more efficiently than liquid water with more absorbed energy, increasing the relative humidity. As shown in Figure 4a, there is more liquid (solid) precipitation produced under clean (polluted) conditions than under polluted (clean) conditions with heavy precipitation case. That's because conversion from cloud droplets to raindrops is more efficient due to higher collision/coalescence efficiency under clean conditions (Albrecht, 1989; Li et al., 2008; Rosenfeld, 1999). Meanwhile, the ice particles are generally larger under polluted conditions once produced (Li et al., 2008), making them survive from evaporation during their falling. The efficiency of evaporation battles with that of condensation, and the aerosol type can affect the result. The temperature and relative humidity can affect the evaporation efficiency, which can both be further influenced by aerosols. As shown in Figure 4b, aerosols can heat the atmosphere due to the presence of

SUN ET AL. 5 of 11

19448007, 2023, 2, Downloaded from https://agupubs.onlinelibrary.wiley.com/doi/10.1029/2022GL102186, Wiley Online Library on [19/01/2023]. See the Terms and Conditions (https://onlinelibrary.wiley.com/terms-and-conditions) on Wiley Online Library for rules of use; OA articles are governed by the applicable Creative Commons Licenses

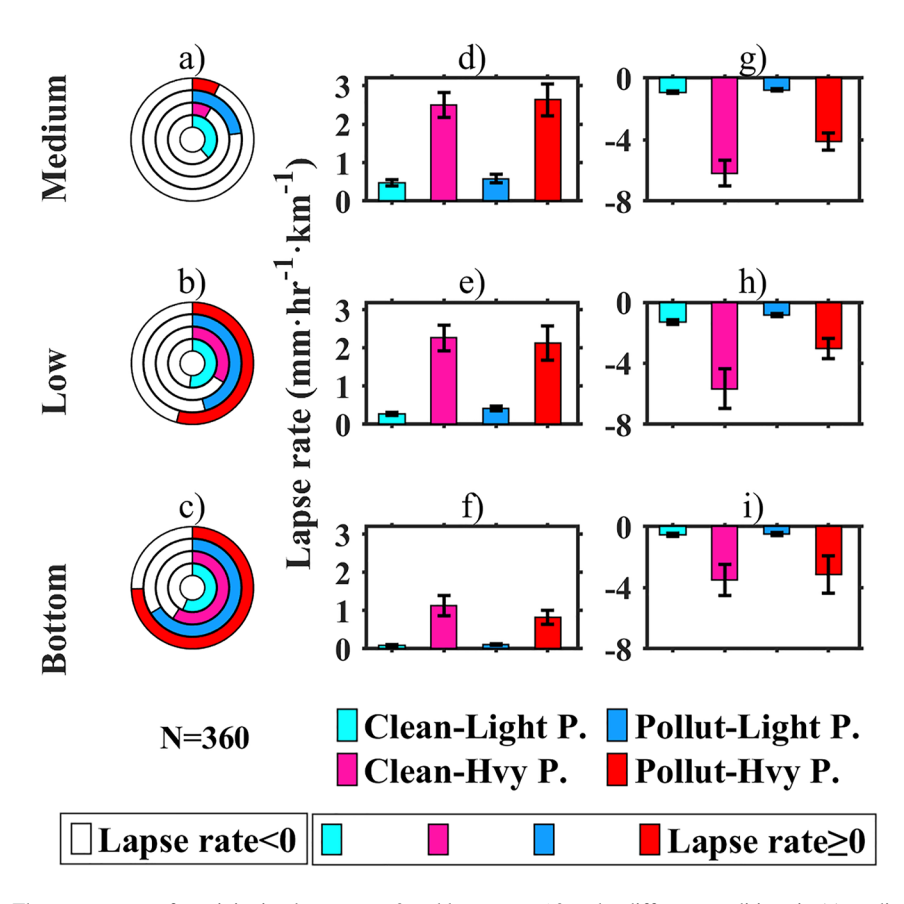


Figure 3. The percentages of precipitation lapse rate  $\geq 0$  and lapse rate  $\leq 0$  under different conditions in (a) medium, (b) low, and (c) bottom layer, respectively. The cyan (blue, roseo, and red) and white circles represent the percentage of lapse rate  $\geq 0$  and lapse rate  $\leq 0$ . From the inner circle to the outer circle, it is clean and light precipitation (Clean-Light P.), clean and heavy precipitation (Clean-Hvy P.), polluted and light precipitation (Pollut-Light P.), polluted and heavy precipitation (Pollut-Hvy P.) in turn. The lapse rate  $\geq 0$  ( $\leq 0$ ) represents precipitation rate decreasing (increasing) in falling. The N represents the sample number. (d−i) the slope of precipitation rate with altitude in Medium, Low, and Bottom Layer, respectively. The average positive slopes (lapse rate  $\geq 0$ ) are shown in (d−f) and negative slopes (lapse rate  $\leq 0$ ) are shown in (g−i).

absorbing aerosols in the study region (He et al., 2020; Sun & Zhao, 2021) and then decrease the relative humidity, leading to strengthened evaporation. The proportion of positive Aerosol Index (AI) is 82% at precipitation location and the proportions with AI values larger at precipitation location than surrounding environment are 64%–69% (Figure 4c), which indicate that absorbing aerosols can be conductive to the generation and development of precipitation. The temperature differences between heavy and light precipitation are obvious at aerosol layer (about 850–925 hPa) as shown in Figure 4d (Li & Han, 2016; Liu M et al., 2019; Wang F. et al., 2018; Wang Y. et al., 2018), which confirms that more aerosol particles can heat the atmosphere further. Figure 4d shows that the temperature is slightly higher under heavy precipitation than under light precipitation. The heavy precipitation may result from stronger convection which is associated with higher near surface air temperature before precipitation. Although higher near-surface atmospheric temperature associated with heavy precipitation would also enhance evaporation efficiency, the relatively weaker temperature difference shown in Figure 4d between heavy and light precipitation under polluted conditions implies that the evaporation should have been strengthened by more aerosol particles.

#### 3.3. A Theoretical Framework to Explain the Observed Relationships

Previous studies have proposed many mechanisms about aerosol effect on precipitation. The positive precipitation-aerosol relationships have been attributed to invigoration effect (e.g., Fan et al., 2018; Rosenfeld et al., 2008). The negative precipitation-aerosol relationships have been ascribed to cloud water competition (Albrecht, 1989; Rosenfeld, 1999), wet scavenging (Grandey et al., 2014), decreased solar radiation by aerosols

SUN ET AL. 6 of 11

19448007, 2023, 2, Downloaded from https://agupubs.onlinelibrary.wiley.com/doi/10.1029/2022GL102186, Wiley Online Library on [19/01/2023]. See the Terms and Conditions (https://onlinelibrary.wiley

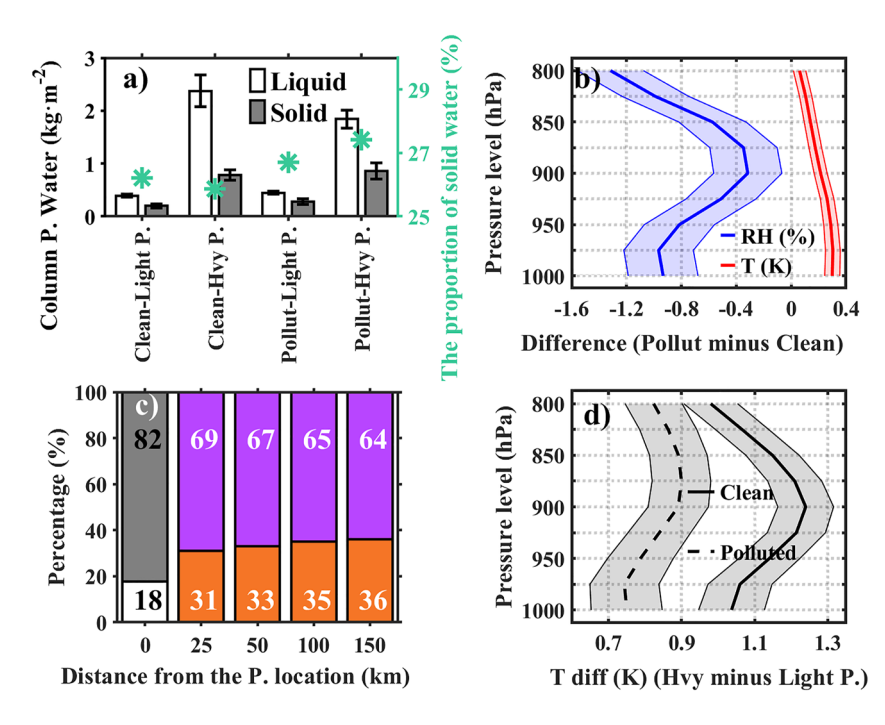


**Figure 4.** (a) The liquid/solid precipitation water in column from GPM (kg m<sup>-2</sup>) under different pollution and near surface precipitation rate conditions. The green starlike dots are the proportion of solid water. (b) The difference of temperature and relative humidity between polluted and clean conditions when precipitation occurs. The blue and red line represent relative humidity and temperature, respectively. (c) The proportion of positive/negative (gray/white histogram) AI at precipitation location and the proportions of positive/negative (purple/orange histogram) AI at D. The D is the difference of AI between at precipitation location and surrounding environment around precipitation location, and the latter is a region within a 25 (50, 100, and 150) km radius around precipitation location. The selected sample number is 377. (d) The temperature difference between heavy and light precipitation cases under clean (solid line) and polluted (dash line) conditions.

(Jiang et al., 2016), evaporation and sublimation of hydrometeors (Dagan et al., 2015; Liu H et al., 2019), and so on. However, these hypotheses are not applicable to our cases. Based on the results shown in Figures 1-4, we propose an explanatory theoretical framework here. The competition between released latent heat and evaporation cooling may explain the boomerang-shape aerosol effect on precipitation-top height. The part of cloud margin is under sub-saturation (Wang et al., 2009) and the evaporation cooling effect sometimes can offset the latent heat released from condensation and then suppress the development of cloud (Fan et al., 2009). The CCN number concentration increases with aerosols from clean to medium pollution conditions, resulting in more cloud droplets and frozen ice particles with enhanced latent heat release (Li et al., 2008). Meanwhile, the condensation or sublimation of cloud droplets don't consume water vapor excessively (Dagan et al., 2015; Fan et al., 2007), which means that the relative humidity on the edge of the cloud has no strong change; the collision-coalescence processes occur after condensation processes and reduce the total superficial area of cloud droplets (Dagan et al., 2015; Freud & Rosenfeld, 2012) and then weaken the evaporation on the edge of the cloud; hence the convective clouds can develop further. Under the polluted conditions, the CCN number concentration increases but the cloud effective radius decreases (shown in Figure S3 in Supporting Information S1) (Kaufman & Fraser, 1997; Kaufman & Nakajima, 1993), which contributes to prolonged condensation or sublimation (Dagan et al., 2015), delayed collision-coalescence processes (Albrecht, 1989; Ross & Phillips, 1957; Squires, 1958; Warner, 1968) and increased total surface cloud droplets aera (Dagan et al., 2015). Hence, there is more (less) latent heat released from condensation (freezing) (Dagan et al., 2015; Seiki & Nakajima, 2014) and more consumed water vapor (Dagan et al., 2015; Li et al., 2008), which implies that the heat absorbed by evaporation is larger than the released latent heat (Jiang et al., 2006; A. Khain et al., 2005; Small et al., 2009; Xue & Feingold, 2006) and then suppresses the development of cloud and precipitation. As a result, the precipitation-top heights are the highest under medium pollution conditions. In other words, the precipitation-top heights increase first and then decrease with increasing aerosol amount.

Under the polluted conditions, the conversion from cloud droplets to raindrops and the process of ice nucleation are hindered. However, the graupel particles will be larger than that under clean conditions once produced

SUN ET AL. 7 of 11

(Li et al., 2008), which can make them survive from evaporation. While under the clean conditions, the cloud droplets are converted into raindrops largely, resulting in more but smaller raindrops than those under polluted conditions due to more efficiently collision/coalescence (Albrecht, 1989; Li et al., 2008; Rosenfeld, 1999). The numerous small raindrops with large superficial area are conductive to evaporation. As a result, the precipitation rates are similar under different pollution conditions. Besides, the absorbing aerosol can create warm and dry conditions to enhance evaporation (shown in Figure 4b).

#### 4. Conclusion and Discussion

Our observation-based analyses reveal that aerosols enhance precipitation-top height first and then suppress it for local scale convective precipitation with ice-phase processes. The turning point occurs at medium aerosol amount. The boomerang-shape effect persists over different atmospheric dynamical and thermodynamical conditions with turning points at similar aerosol amount. The high CAPE-high PWV-low WS-high RH generally make the precipitation-top height higher. Strong evaporation modifies the response of precipitation to aerosol from cloud base to the surface. Near surface precipitation rate shows no significant responses to aerosol and precipitation-top height. The atmospheric environment temperature, relative humidity, and aerosol amount affect evaporation of precipitation, which most likely plays a more important role than other factors in determining near surface precipitation rate.

A physical framework is proposed in the present study to explain the findings above. The key lies in the competition between latent heat released from condensation and freezing processes and energy absorbed by evaporation process. From clean to medium pollution conditions, the released latent heat by condensation and freezing is more than the energy absorbed by evaporation, which enhances the precipitation-top height. In contrast, the latent heat released is less than the energy absorbed from medium to heavy pollution conditions, which suppresses the precipitation-top height. The size and number of raindrops strongly regulate the evaporation efficiency and then precipitation rate. The small and numerous droplets are conductive to evaporation under the subsaturated conditions. Moreover, due to the accumulated absorbing aerosols at low troposphere, the near surface precipitation rate is largely controlled by evaporation, resulting from increased temperature and decreased relative humidity.

In this study, we provide a holistic perspective to investigate cloud and precipitation simultaneously throughout the whole vertical processes of precipitation. While this study only focuses on the North China Plain, similar results about the aerosol impacts on convective precipitation can be expected over other regions with sufficient aerosol amount and similar aerosol types. In-depth modeling simulations will be done, and observational analyses can be extended in future to cover more regions with increased sample volume.

#### **Data Availability Statement**

The details of the hourly precipitation data from the China Merged Precipitation Analysis Version 1.0 product can be found from https://www.ckcest.cn/default/es3/detail/4004/dw\_dataset/C92AF495DE300001E3 27C1BD56401982 (last access: 22 November 2022) (Shen et al., 2014). The PM<sub>2.5</sub> mass concentration data used in this article can be obtained from https://zenodo.org/record/6950751/. The DPR Level-2A product from the Global Precipitation Measurement (GPM) (Iguchi & Meneghini, 2021) mission can be downloaded from https://doi.org/10.5067/GPM/DPR/GPM/2A/07. NCEP (https://doi.org/10.5065/D6M043C6) reanalysis data sets. MERRA-2 (http://doi.org/10.5067/G0U6NGQ3BLE0). The ultraviolet AI from the Ozone Monitoring Instrument (OMI) onboard the Aura satellite is from https://doi.org/10.5067/Aura/OMI/DATA3004 (Deborah & Veefkind, 2012). The Aerosol Robotic Network (AERONET) datum are from https://aeronet.gsfc.nasa. gov/cgi-bin/draw\_map\_display\_aod\_v3 and https://aeronet.gsfc.nasa.gov/cgi-bin/draw\_map\_display\_inv\_v3. Himawari-8 cloud mask product is obtained from http://www.eorc.jaxa.jp/ptree/index.html. The ERA5 product is obtained from https://doi.org/10.24381/cds.bd0915c6 (Hersbach et al., 2018).

National Natural Science Foundation of China (42230601, 41925022), the Ministry of Science and Technology of China National Key Research and Development Program (2019YFA0606803). Yue Sun is supported by the Beijing Normal University Interdisciplinary Research Foundation for the First-Year Doctoral Candidates (BNUXKJC2127). Yuan Wang acknowledges the support from U.S. National Science Foundation (AGS-2103714).

Chuanfeng Zhao is supported by the

Acknowledgments

#### References

Ackerman, A. S., Toon, O. B., Stevens, D. E., Heymsfield, A. J., Ramanathan, V. V., & Welton, E. J. (2000). Reduction of tropical cloudiness by soot. Science, 288(5468), 1042-1047. https://doi.org/10.1126/science.288.5468.1042 Albrecht, B. A. (1989). Aerosols, cloud microphysics, and fractional cloudiness. Science, 245(4923), 1227-1230. https://doi.org/10.1126/scien ce.245.4923.1227

SUN ET AL. 8 of 11

- Andreae, M. O., Rosenfeld, D., Artaxo, P., Costa, A. A., Frank, G. P., Longo, K. M., & Silva-Dias, M. A. F. (2004). "Smoking" rain clouds over the Amazon. Science, 303(5662), 1337–1342. https://doi.org/10.1126/science.1092779
- Chen, T., Li, Z., Kahn, R. A., Zhao, C., Rosenfeld, D., Guo, J., et al. (2021). Potential impact of aerosols on convective clouds revealed by Himawari-8 observations over different terrain types in eastern China. *Atmospheric Chemistry and Physics*, 21(8), 6199–6220. https://doi.org/10.5194/acp-21-6199-2021
- Chen, T. M., Guo, J. P., Li, Z. Q., Zhao, C., Liu, H., Cribb, M., et al. (2016). A CloudSat perspective on the cloud climatology and its association with aerosol perturbations in the vertical over Eastern China. *Journal of the Atmospheric Sciences*, 73(9), 3599–3616. https://doi.org/10.1175/JAS-D-15-0309.1
- Dagan, G., Koren, I., & Altaratz, O. (2015). Competition between core and periphery-based processes in warm convective clouds From invigoration to suppression. Atmospheric Chemistry and Physics, 15(5), 2749–2760. https://doi.org/10.5194/acp-15-2749-2015
- Deborah, S.-Z., & Veefkind, P. (2012). OMI/Aura multi-wavelength aerosol optical depth and single scattering albedo L3 1 day best pixel in 0.25 degree v 0.25 degree V3, NASA Goddard Space Flight Center. Goddard Earth Sciences Data and Information Services Center (GES DISC).
- Fan, H., Wang, Y., Zhao, C., Yang, Y., Yang, X., Sun, Y., & Jiang, S. (2021). The role of primary emission and transboundary transport in the air quality changes during and after the COVID-19 lockdown in China. Geophysical Research Letters, 48(7), e2020GL091065. https://doi. org/10.1029/2020GL091065
- Fan, J., Yuan, T., Comstock, J. M., Ghan, S., Khain, A., Leung, L. R., et al. (2009). Dominant role by vertical wind shear in regulating aerosol effects on deep convective clouds. *Journal of Geophysical Research*, 114(D22), D22206. https://doi.org/10.1029/2009JD012352
- Fan, J., Zhang, R., Li, G., & Tao, W.-K. (2007). Effects of aerosols and relative humidity on cumulus clouds. *Journal of Geophysical Research*, 112(D14), D14204. https://doi.org/10.1029/2006JD008136
- Fan, J. W., Rosenfeld, D., Zhang, Y. W., Giangrande, S. E., Li, Z. Q., Machado, L. A. T., et al. (2018). Substantial convection and precipitation enhancements by ultrafine aerosol particles. *Science*, 359(6374), 411–418. https://doi.org/10.1126/science.aan8461
- Freud, E., & Rosenfeld, D. (2012). Linear relation between convective cloud drop number concentration and depth for rain initiation. *Journal of Geophysical Research*, 117(D2), D02207. https://doi.org/10.1029/2011JD016457
- Garrett, T. J., & Zhao, C. (2006). Increased Arctic cloud longwave emissivity associated with pollution from mid-latitudes. *Nature*, 440(7085), 787–789. https://doi.org/10.1038/nature04636
- Grandey, B. S., Gururaj, A., Stier, P., & Wagner, T. M. (2014). Rainfall-aerosol relationships explained by wet scavenging and humidity. *Geophysical Research Letters*, 41(15), 5678–5684. https://doi.org/10.1002/2014GL060958
- Gryspeerdt, E., & Stier, P. (2012). Regime-based analysis of aerosol-cloud interactions. *Geophysical Research Letters*, 39(21), L21802. https://
- doi.org/10.1029/2012GL053221
  Gryspeerdt, E., Stier, P., & Partridge, D. G. (2014). Satellite observations of cloud regime development: The role of aerosol processes. *Atmos-*
- pheric Chemistry and Physics, 14(3), 1141–1158. https://doi.org/10.5194/acp-14-1141-2014
  Guo, J., Deng, M., Fan, J., Li, Z., Chen, O., Zhai, P., et al. (2014). Precipitation and air pollution at mountain and plain stations in northern
- Guo, J., Deng, M., Fan, J., Li, Z., Chen, Q., Zhai, P., et al. (2014). Precipitation and air pollution at mountain and plain stations in northern China: Insights gained from observations and modeling. *Journal of Geophysical Research: Atmospheres*, 119(8), 4793–4807. https://doi. org/10.1002/2013JD021161
- Guo, J., Deng, M., Lee, S. S., Wang, F., Li, Z., Zhai, P., et al. (2016). Delaying precipitation and lightning by air pollution over the Pearl River Delta. Part I: Observational analyses. *Journal of Geophysical Research: Atmospheres*, 121(11), 6472–6488. https://doi.org/10.1002/2015JD023257
- Guo, J., Su, T., Chen, D., Wang, J., Li, Z., Lv, Y., et al. (2019). Declining summertime local-scale precipitation frequency over China and the United States, 1981-2012: The disparate roles of aerosols. *Geophysical Research Letters*, 46(22), 13281–13289. https://doi.org/ 10.1029/2019GL085442
- Guo, X. L., Fu, D. H., Guo, X., & Zhang, C. M. (2014). A case study of aerosol impacts on summer convective clouds and precipitation over northern China. Atmospheric Research, 142, 142–157. https://doi.org/10.1016/j.atmosres.2013.10.006
- Hamada, A., & Takayabu, Y. N. (2015). Improvements in detection of light precipitation with the global precipitation measurement dual-frequency precipitation radar (GPM DPR). *Journal of Atmospheric and Oceanic Technology*, 33(4), 653–667. https://doi.org/10.1175/JTECH-D-15-0007-1
- Hammer, M. S., Martin, R. V., Li, C., Torres, O., Manning, M., & Boys, B. L. (2018). Insight into global trends in aerosol composition from 2005 to 2015 inferred from the OMI Ultraviolet Aerosol Index. Atmospheric Chemistry and Physics, 18(11), 8097–8112. https://doi.org/10.5194/acp-18-8097-2018
- acp-18-809/-2018

  Han, X., Zhao, B., Lin, Y., Chen, Q., Shi, H., Jiang, Z., et al. (2022). Type-dependent impact of aerosols on precipitation associated with deep convective cloud over East Asia. *Journal of Geophysical Research: Atmospheres*, 127(2), e2021JD036127. https://doi.org/10.1029/2021JD036127
- He, X., Lu, C. S., & Zhu, J. (2020). A study of the spatiotemporal variation in aerosol types and their radiation effect in China. Acta Scientiae Circumstantiae, 40(11), 4070–4080. (in Chinese). https://doi.org/10.13671/j.hjkxxb.2020.0100
- Hersbach, H., Bell, B., Berrisford, P., Biavati, G., Horányi, A., Muñoz Sabater, J., et al. (2018). ERA5 hourly data on pressure levels from 1959 to present. Copernicus climate change service (C3S) climate data store (CDS).
- Iguchi, T., & Meneghini, R. (2021). GPM DPR precipitation profile L2A 1.5 hours 5 km V07, Greenbelt, MD. Goddard Earth Sciences Data and Information Services Center (GES DISC).
- Jiang, H., Xue, H., Teller, A., Feingold, G., & Levin, Z. (2006). Aerosol effects on the lifetime of shallow cumulus. *Geophysical Research Letters*, 33(14), L14806. https://doi.org/10.1029/2006GL026024
- Jiang, J. H., Su, H., Huang, L., Wang, Y., Massie, S., Zhao, B., et al. (2018). Contrasting effects on deep convective clouds by different types of aerosols. Nature Communications, 9(1), 3874. https://doi.org/10.1038/s41467-018-06280-4
- Jiang, M., Li, Z., Wan, B., & Cribb, M. (2016). Impact of aerosols on precipitation from deep convective clouds in eastern China. *Journal of Geophysical Research: Atmospheres*, 12(16), 9607, 9620. https://doi.org/10.1002/2015ID024246
- Geophysical Research: Atmospheres, 121(16), 9607–9620. https://doi.org/10.1002/2015JD024246

  Kaufman, Y. J., & Fraser, R. S. (1997). The effect of smoke particles on clouds and climate forcing. Science, 277(5332), 1636–1639. https://
- Kaufman, Y. J., & Nakajima, T. (1993). Effect of Amazon smoke on cloud microphysics and albedo-analysis from satellite imagery. *Journal of Applied Meteorology and Climatology*, 32(4), 729–744. https://doi.org/10.1175/1520-0450(1993)032<0729:EOASOC>2.0.CO;2
- Khain, A., Rosenfeld, D., & Pokrovsky, A. (2005). Aerosol impact on the dynamics and microphysics of deep convective clouds. *Quarterly Journal of the Royal Meteorological Society*, 131(611), 2639–2663. https://doi.org/10.1256/qj.04.62
- Khain, A. P. (2009). Notes on state-of-the-art investigations of aerosol effects on precipitation: A critical review. Environmental Research Letters, 4(1), 15004. https://doi.org/10.1088/1748-9326/4/1/015004
- Koren, I., Altaratz, O., Remer, L. A., Feingold, G., Martins, J. V., & Heiblum, R. H. (2012). Aerosol-induced intensification of rain from the tropics to the mid-latitudes. *Nature Geoscience*, 5(2), 118–122. https://doi.org/10.1038/ngeo1364

SUN ET AL. 9 of 11

doi.org/10.1126/science.277.5332.1636

- Koren, I., Kaufman, Y. J., Rosenfeld, D., Remer, L. A., & Rudich, Y. (2005). Aerosol invigoration and restructuring of Atlantic convective clouds. Geophysical Research Letters, 32(14), L14828. https://doi.org/10.1029/2005GL023187
- Koren, I., Martins, J. V., Remer, L. A., & Afargan, H. (2008). Smoke invigoration versus inhibition of clouds over the Amazon. *Science*, 321(5891), 946–949. https://doi.org/10.1126/science.1159185
- Kotsuki, S., Terasaki, K., & Miyoshi, T. (2014). GPM/DPR precipitation compared with a 3.5 km resolution NICAM simulation. SOLA, 10(0), 204–209. https://doi.org/10.2151/sola.2014-043
- Lee, J., Kim, J., Song, C. H., Kim, S. B., Chun, Y., Sohn, B. J., & Holben, B. (2010). Characteristics of aerosol types from AERONET sunphotometer measurements. Atmospheric Environment, 44(26), 3110–3117. https://doi.org/10.1016/j.atmosenv.2010.05.035
- Lee, S. S., Feingold, G., & Chuang, P. Y. (2015). Effect of aerosol on cloud-environment interactions in trade cumulus. *Journal of the Atmospheric Sciences*, 69(12), 3607–3632. https://doi.org/10.1175/JAS-D-12-026.1
- Li, G., Wang, Y., & Zhang, R. (2008). Implementation of a two-moment bulk microphysics scheme to the WRF model to investigate aerosol-cloud interaction. *Journal of Geophysical Research*, 113(D15), D15211. https://doi.org/10.1029/2007JD009361
- Li, J., & Han, Z. (2016). Aerosol vertical distribution over east China from RIEMS-Chem simulation in comparison with CALIPSO measurements. Atmospheric Environment, 143, 177–189. https://doi.org/10.1016/j.atmosenv.2016.08.045
- Li, M., Letu, H., Peng, Y., Ishimoto, H., Lin, Y., Nakajima, T. Y., et al. (2022). Investigation of ice cloud modeling capabilities for the irregularly shaped Voronoi ice scattering models in climate simulations. Atmospheric Chemistry and Physics, 22(7), 4809–4825. https://doi.org/10.5194/acp-22-4809-2022
- Lin, J. C., Matsui, T., Pielke, R. A., & Kummerow, C. D. (2006). Effects of biomass-burning-derived aerosols on precipitation and clouds in the Amazon basin: A satellite-based empirical study. *Journal of Geophysical Research*, 111(D19), D19204. https://doi.org/10.1029/2005JD006884
- Liu, H., Guo, J. P., Koren, I., Altaratz, O., Dagan, G., Wang, Y., et al. (2019). Non-monotonic aerosol effect on precipitation in convective clouds over tropical oceans. *Scientific Reports*, 9(1), 7809. https://doi.org/10.1038/s41598-019-44284-2
- Liu, M., Lin, J., Boersma, K. F., Pinardi, G., Wang, Y., Chimot, J., et al. (2019). Improved aerosol correction for OMI tropospheric NO2 retrieval over East Asia: Constraint from CALIOP aerosol vertical profile. *Atmospheric Measurement Techniques*, 12(1), 1–21. https://doi.org/10.5194/am
- Mülmenstädt, J., Sourdeval, O., Delanoë, J., & Quaas, J. (2015). Frequency of occurrence of rain from liquid-mixed-and ice-phase clouds derived from A-Train satellite retrievals. *Geophysical Research Letters*, 42(15), 6502–6509. https://doi.org/10.1002/2015GL064604
- Pan, Z., Rosenfeld, D., Zhu, Y., Mao, F., Gong, W., Zang, L., & Lu, X. (2021). Observational quantification of aerosol invigoration for deep convective cloud lifecycle properties based on geostationary satellite. *Journal of Geophysical Research: Atmospheres*, 126(9), e2020JD034275. https://doi.org/10.1029/2020JD034275
- Qian, Y., Gong, D., Fan, J., Leung, L. R., Bennartz, R., Chen, D., & Wang, W. (2009). Heavy pollution suppresses light rain in China: Observations and modeling. *Journal of Geophysical Research*, 114, D00K02. https://doi.org/10.1029/2008JD011575
- Ramanathan, V., Crutzen, P. J., Kiehl, J. T., & Rosenfeld, D. (2001). Aerosols, climate, and the hydrological cycle. Science, 294(5549), 2119–2124. https://doi.org/10.1126/science.1064034
- Rosenfeld, D. (1999). TRMM observed first direct evidence of smoke from forest fires inhibiting rainfall. *Geophysical Research Letters*, 26(20), 3105–3108. https://doi.org/10.1029/1999GL006066
- Rosenfeld, D., Lohmann, U., Raga, G. B., O'Dowd, D. D., Kulmala, M., Fuzzi, S., et al. (2008). Flood or drought: How do aerosols affect precipitation? *Science*, 321(5894), 1309–1313. https://doi.org/10.1126/science.1160606
- Ross, G., & Phillips, B. B. (1957). An experimental investigation of the effect of air pollution on the initiation of rain. *Journal of the Atmospheric Sciences*, 14(3), 272–280. https://doi.org/10.1175/1520-0469(1957)0142.0.CO;2
- Seiki, T., & Nakajima, T. (2014). Aerosol effects of the condensation process on a convective cloud simulation. *Journal of the Atmospheric Sciences*, 71(2), 833–853. https://doi.org/10.1175/JAS-D-12-0195.1
- Shen, Y., Zhao, P., Pan, Y., & Yu, J. (2014). A high spatiotemporal gauge-satellite merged precipitation analysis over China. *Journal of Geophysical Research: Atmospheres*, 119(6), 3063–3075. https://doi.org/10.1002/2013JD020686
- Small, J. D., Chuang, P. Y., Feingold, G., & Jiang, H. (2009). Can aerosol decrease cloud lifetime? Geophysical Research Letters, 36(16), L16806. https://doi.org/10.1029/2009GL038888
- Squires, P. (1958). The microstructure and colloidal stability of warm clouds. Tellus, 10(2), 262–271. https://doi.org/10.1111/j.2153-3490.1 958.tb02012.x
- Sun, J., Wang, Z., Zhou, W., Xie, C., Wu, C., Chen, C., et al. (2022). Measurement report: Long-term changes in black carbon and aerosol optical properties from 2012 to 2020 in Beijing, China. Atmospheric Chemistry and Physics, 22(1), 561–575. https://doi.org/10.5194/acp-22-561-2022
- Sun, Y., Dong, X., Cui, W., Zhou, Z., Fu, Z., Zhou, L., et al. (2020). Vertical structures of typical Meiyu precipitation events retrieved from GPM-DPR. *Journal of Geophysical Research: Atmospheres*, 125(1), e2019JD031466. https://doi.org/10.1029/2019JD031466
- Sun, Y., & Zhao, C. (2020). Influence of Saharan dust on the large-scale meteorological environment for development of tropical cyclone over North Atlantic Ocean Basin. *Journal of Geophysical Research: Atmospheres*, 125(23), e2020JD033454, https://doi.org/10.1029/2020JD033454
- Sun, Y., & Zhao, C. (2021). Distinct impacts on precipitation by aerosol radiative effect over three different megacity regions of eastern China. Atmospheric Chemistry and Physics, 21(21), 16555–16574. https://doi.org/10.5194/acp-21-16555-2021
- Swain, D. L., Langenbrunner, B., Neelin, J. D., & Hall, A. (2018). Increasing precipitation volatility in twenty-first-century California. *Nature Climate Change*, 8(5), 427–433. https://doi.org/10.1038/s41558-018-0140-y
- Tariq, S., & Ali, M. (2015). Spatio-temporal distribution of absorbing aerosols over Pakistan retrieved from OMI onboard Aura satellite. Atmospheric Pollution Research, 6(2), 254–266. https://doi.org/10.5094/APR.2015.030
- Twomey, S. (1977). The influence of pollution on the shortwave albedo of clouds. *Journal of the Atmospheric Sciences*, 34(7), 1149–1152. htt ps://doi.org/10.1175/1520-0469(1977)034<1149:TIOPOT>2.0.CO;2
- Wang, F., Li, Z., Ren, X., Jiang, Q., He, H., Dickerson, R. R., et al. (2018). Vertical distributions of aerosol optical properties during the spring 2016 ARIAs airborne campaign in the North China Plain. Atmospheric Chemistry and Physics, 18(12), 8995–9010. https://doi.org/10.5194/acp-18-8995-2018
- Wang, L., Qian, Y., Leung, L. R., Chen, X., Sarangi, C., Lu, J., et al. (2021). Multiple metrics informed projections of future precipitation in China. Geophysical Research Letters, 48(18), e2021GL093810. https://doi.org/10.1029/2021GL093810
- Wang, R., Tian, W. S., Chen, F. J., Wei, D., Luo, J. L., Tian, H. Y., & Zhang, J. (2021). Analysis of convective and stratiform precipitation characteristics in the summers of 2014–2019 over Northwest China based on GPM observations. *Atmospheric Research*, 262, 105762. https://doi.org/10.1016/j.atmosres.2021.105762
- Wang, Y., Khalizov, A. F., Levy, M., & Zhang, R. Y. (2013). New directions: Light absorbing aerosols and their atmospheric impacts. Atmospheric Environment, 81, 713–715. https://doi.org/10.1016/j.atmosenv.2013.09.034

SUN ET AL. 10 of 11

- Wang, Y., Ma, P.-L., Jiang, J., Su, H., & Rasch, P. (2016). Towards reconciling the influence of atmospheric aerosols and greenhouse gases on light precipitation changes in Eastern China. *Journal of Geophysical Research Atmospheres*, 121(10), 5878–5887. https://doi.org/10.1002/2016JD024845
- Wang, Y., Vogel, J. M., Lin, Y., Pan, B. W., Hu, J. X., Liu, Y. G., et al. (2018). Aerosol microphysical and radiative effects on continental cloud ensembles. *Advances in Atmospheric Sciences*, 35(2), 234–247. https://doi.org/10.1007/s00376-017-7091-5
- Wang, Y. G., Geerts, B., & French, J. (2009). Dynamics of the cumulus cloud margin: An observational study. *Journal of the Atmospheric Sciences*, 66(12), 3660–3677. https://doi.org/10.1175/2009JAS3129.1
- Warner, J. (1968). A reduction in rainfall associated with smoke from sugar-cane fires-an inadvertent weather modification? *Journal of Applied Meteorology and Climatology*, 7(2), 247–251. https://doi.org/10.1175/1520-0450(1968)007<0247:ARIRAW>2.0.CO;2
- Wilks, D. S. (2011). Statistical methods in the atmospheric sciences. Academic Press.
- Xiao, Z. S., Zhu, S. B., Miao, Y. C., Yu, Y., & Che, H. Z. (2022). On the relationship between convective precipitation and aerosol pollution in North China Plain during autumn and winter. Atmospheric Research, 271, 106120. https://doi.org/10.1016/j.atmosres.2022.106120
- Xue, H., & Feingold, G. (2006). Large-eddy simulations of trade wind cumuli: Investigation of aerosol indirect effects. *Journal of the Atmospheric Sciences*, 63(6), 1605–1622. https://doi.org/10.1175/JAS3706.1
- Yang, X., Li, Z., Liu, L., Zhou, L., Cribb, M., & Zhang, F. (2016). Distinct weekly cycles of thunderstorms and a potential connection with aerosol type in China. Geophysical Research Letters, 43(16), 8760–8768. https://doi.org/10.1002/2016GL070375
- Yang, X., Zhou, L., Zhao, C., & Yang, J. (2018). Impact of aerosols on tropical cyclone-induced precipitation over the mainland of China. Climatic Change, 148(1–2), 173–185. https://doi.org/10.1007/s10584-018-2175-5
- Yang, Y., Zhao, C., Wang, Q., Cong, Z., Yang, X., & Fan, H. (2021c). Aerosol characteristics at the three poles of the Earth as characterized by cloud–aerosol lidar and infrared pathfinder satellite observations. Atmospheric Chemistry and Physics, 21(6), 4849–4868. https://doi. org/10.5194/acp-21-4849-2021
- Yang, Y., Zhao, C., Wang, Y., Zhao, X., Sun, W., Yang, J., et al. (2021b). Multi-source data based investigation of aerosol-cloud interaction over the North China Plain and north of the Yangtze Plain. *Journal of Geophysical Research: Atmospheres*, 126(19), e2021JD035609. https://doi.org/10.1029/2021JD035609
- Yang, Y. J., Wang, R., Chen, F. J., Liu, C., Bi, X. Y., & Huang, M. (2021a). Synoptic weather patterns modulate the frequency, type and vertical structure of summer precipitation over Eastern China: A perspective from GPM observations. Atmospheric Research, 249, 105342. https://doi.org/10.1016/j.atmosres.2020.105342
- Zhang, A., & Fu, Y. (2018). Life cycle effects on the vertical structure of precipitation in East China measured by Himawari-8 and GPM DPR. Monthly Weather Review, 146(7), 2183–2199. https://doi.org/10.1175/MWR-D-18-0085.1
- Zhang, F., Wang, Y., Peng, J. F., Chen, L., Sun, Y. L., Duan, L., et al. (2020). An unexpected catalyst dominates formation and radiative forcing of regional haze. Proceedings of the National Academy of Sciences of the United States of America, 117(8), 3960–3966. https://doi.org/10.1073/pngs.1919343117
- Zhang, W. X., Furtado, K., Wu, P. L., Zhou, T. J., Chadwick, R., Marzin, C., et al. (2021). Increasing precipitation variability on daily-to-multiyear time scales in a warmer world. Science Advances, 7(31), eabf8021. https://doi.org/10.1126/sciadv.abf8021
- Zhao, C., & Garrett, T. J. (2008). Ground-based remote sensing of precipitation in the Arctic. *Journal of Geophysical Research*, 113(D14), D14204. https://doi.org/10.1029/2007JD009222
- Zhao, C., Lin, Y., Wu, F., Wang, Y., Li, Z., Rosenfeld, D., & Wang, Y. (2018). Enlarging rainfall area of tropical cyclones by atmospheric aerosols. Geophysical Research Letters, 45(16), 8604–8611. https://doi.org/10.1029/2018GL079427
- Zhao, C., Tie, X., & Lin, Y. (2006). A possible positive feedback of reduction of precipitation and increase in aerosols over eastern central China. Geophysical Research Letters, 33(11), L11814. https://doi.org/10.1029/2006GL025959

SUN ET AL. 11 of 11